

Carbon isotope excursions in paleosol carbonate

H. A. Abels et al.

Carbon isotope excursions in paleosol carbonate marking five early Eocene hyperthermals in the Bighorn Basin, Wyoming

H. A. Abels¹, V. Lauretano¹, A. van Yperen^{1,*}, T. Hopman^{1,**}, J. C. Zachos², L. J. Lourens¹, P. D. Gingerich³, and G. J. Bowen⁴

¹Department of Earth Sciences, Utrecht University, Budapestlaan 4, 3584 CD, Utrecht, the Netherlands

²Department of Earth and Planetary Sciences, University of California Santa Cruz, 1156 High Street, Santa Cruz, CA 95064, USA

³Department of Earth and Environmental Sciences, University of Michigan, Ann Arbor, Michigan 48109, USA

⁴Department of Geology and Geophysics, University of Utah, Salt Lake City, UT 84112, USA

* now at: Enres International, Euclideslaan 201, 3584 BS, Utrecht, the Netherlands

** now at: PanTerra, Weversbaan 1–3, 2352 BZ, Leiderdorp, the Netherlands

Title Page

Abstract

Introduction

Conclusions

References

Tables

Figures



Back

Close

Full Screen / Esc

Printer-friendly Version

Interactive Discussion



Received: 16 April 2015 – Accepted: 17 April 2015 – Published: 18 May 2015

Correspondence to: H. A. Abels (h.a.abels@uu.nl)

Published by Copernicus Publications on behalf of the European Geosciences Union.

CPD

11, 1857–1885, 2015

Carbon isotope excursions in paleosol carbonate

H. A. Abels et al.

[Title Page](#)

[Abstract](#)

[Introduction](#)

[Conclusions](#)

[References](#)

[Tables](#)

[Figures](#)



[Back](#)

[Close](#)

[Full Screen / Esc](#)

[Printer-friendly Version](#)

[Interactive Discussion](#)



Abstract

Transient greenhouse warming events in the Paleocene and Eocene were associated with the addition of isotopically-light carbon to the exogenic atmosphere–ocean carbon pool, leading to substantial environmental and biotic change. The magnitude of an accompanying carbon isotope excursion (CIE) can be used to constrain both the sources and amounts of carbon released during an event, as well as to correlate marine and terrestrial records with high precision. The Paleocene Eocene Thermal Maximum (PETM) is well documented, but CIE records for the subsequent warming events are still rare especially from the terrestrial realm.

Here, we provide new CIE records for two of the smaller hyperthermal events, I1 and I2, in paleosol carbonate, as well as two additional records of ETM2 and H2 in the Bighorn Basin. Stratigraphic comparison of this expanded, high-resolution terrestrial carbon isotope record to the deep-sea benthic foraminifera records from ODP Sites 1262 and 1263, Walvis Ridge, in the southern Atlantic Ocean corroborates that the Bighorn Basin fluvial sediments record global atmospheric change. The stratigraphic thicknesses of the eccentricity-driven hyperthermals in these archives are in line with precession-forcing of the 7 m thick fluvial overbank-avulsion sedimentary cycles. Using the CALMAG bulk oxide mean annual precipitation proxy, we reconstruct similar or slightly wetter than background soil moisture contents during the four younger hyperthermals, in contrast to drying observed during the PETM. Soil carbonate CIEs vary in magnitude proportionally with the marine CIEs for the four smaller early Eocene hyperthermals. This relationship breaks down for the PETM, with the soil carbonate CIE $\sim 2\text{--}4\%$ less than expected if all five linearly relate to marine CIEs. If the PETM CO_2 forcing was similar but scaled to the younger hyperthermals, photosynthetic isotope fractionation or soil environmental factors are needed to explain this anomaly. We use sensitivity testing of experimentally determined photosynthetic isotope discrimination relationships to show that factors other than the recently demonstrated $p\text{CO}_2$ sensitivity of C_3 plants carbon isotope fractionation are required to explain this anomaly.

Carbon isotope excursions in paleosol carbonate

H. A. Abels et al.

Title Page

Abstract

Introduction

Conclusions

References

Tables

Figures



Back

Close

Full Screen / Esc

Printer-friendly Version

Interactive Discussion



1 Introduction

During the late Paleocene and early Eocene around 60 to 50 million years ago massive amounts of carbon were released in pulses into the ocean–atmosphere exogenic carbon pool causing a series of transient global warming events, known as hyperthermals (Kennett and Stott, 1991; Cramer et al., 2003; Zachos et al., 2005; Lourens et al., 2005). These events represent the best paleo-analogs for current greenhouse gas warming, despite the very different background climatic, atmospheric, and geographic conditions, and potentially different time scales on which they occurred (Bowen et al., 2006, 2015; Zachos et al., 2008; Cui et al., 2011). The largest of these hyperthermals, the Paleocene–Eocene Thermal Maximum (PETM) at 56 million years ago, is known to have caused severe climatic and marine and terrestrial biotic change (Kennett and Stott, 1991; Koch et al., 1992), reviewed in McInerney and Wing (2011). Recently, records of the secondary hyperthermals (i.e., ETM-2, H1-2, I1-2) became available (Cramer et al., 2003; Lourens et al., 2005; Nicolo et al., 2007), while their environmental and biotic impact has yet to be resolved (Sluijs et al., 2009; Stap et al., 2010a, b; Abels et al., 2012).

All hyperthermals have a distinct geochemical signature, a negative carbon isotope excursion, indicating that the carbon released to the exogenic carbon pool during these events had a dominant biogenic origin (Dickens, 1995). The potential biogenic sources range from plant material to methane. With the carbon isotope excursions, carbon cycle models are used to identify the carbon source(s) and the mass of carbon release. This can be achieved by several approaches, for example quantifying ocean acidification, or $p\text{CO}_2$ by proxy, either direct (e.g., epsilon p) or indirect (e.g., SST) (Dickens, 2000; Bowen et al., 2004; Ridgwell, 2007; Panchuk et al., 2008; Zeebe et al., 2009), though the uncertainty with these approaches is large (Sexton et al., 2011; DeConto et al., 2012; Dickens, 2011). As a start, it is crucial to know the exact size of the carbon isotope excursions (CIEs) in the global exogenic carbon pool during hyperthermal events.

CPD

11, 1857–1885, 2015

Carbon isotope excursions in paleosol carbonate

H. A. Abels et al.

Title Page

Abstract

Introduction

Conclusions

References

Tables

Figures



Back

Close

Full Screen / Esc

Printer-friendly Version

Interactive Discussion



This requires an understanding of the factors fractionation of C-isotopes between the substrate reservoirs and organic and carbonate proxies (Sluijs and Dickens, 2012).

Paleosol or pedogenic carbonate is precipitated from CO₂ that stems from respiration of roots and plant litter in the soil and from atmospheric CO₂ diffusing into the soil. Plant CO₂ from C₃ plants is typically fractionated by -24 to -28‰ compared to atmospheric CO₂. Paleosol carbonate is a mix of both isotopically-distinct sources and therefore registers values between -7 and -11‰ in non-hyperthermal conditions in Paleogene soils covered by C₃ vegetation. Paleosol carbonate registers the atmospheric carbon isotope excursions related to the Paleocene–Eocene Thermal Maximum (PETM), though amplified with respect to marine carbonate (Bowen et al., 2004). This has been explained by increased soil productivity and humidity during the hyperthermal events (Bowen et al., 2004; Bowen and Bowen, 2008) and by changing plant communities (Smith et al., 2007).

In a recent study, the scale of the carbon isotope anomalies associated with ETM2 and H2 were characterized in paleosol carbonate, allowing for comparison of the terrestrial amplification of the CIEs relative to the PETM (Abels et al., 2012). An apparent linear scaling of the marine and terrestrial carbon isotope excursions for the PETM, ETM2 and H2 events was found not to cross the origin and the carbon isotope behavior for the smaller (I1 and I2) events remained uncertain. These comparisons are complicated, however, by shifting background conditions between the events, especially so for the PETM and the younger smaller hyperthermals, which are separated by close to 2 million years at a time when gradual greenhouse warming was occurring (Zachos et al., 2008). Nevertheless, the approach introduced by Abels et al. (2012) offers a reasonable approach to leveraging the multi-proxy CIE data for the Paleogene hyperthermal events to characterize patterns of CIE amplification and potential environmental change relationships among events.

Here, we extend the existing record of three hyperthermals from the Bighorn Basin with data documenting two new CIEs. We further produce two parallel records of the ETM2 and H2 CIEs and analyze bulk oxides in thick (> 0.75 m) soils to reconstruct soil

Carbon isotope excursions in paleosol carbonate

H. A. Abels et al.

[Title Page](#)

[Abstract](#)

[Introduction](#)

[Conclusions](#)

[References](#)

[Tables](#)

[Figures](#)



[Back](#)

[Close](#)

[Full Screen / Esc](#)

[Printer-friendly Version](#)

[Interactive Discussion](#)



moisture values through these greenhouse-warming events. We compare our records with the new benthic foraminiferal records generated for Ocean Drilling Program Site 1263 at Walvis Ridge, Atlantic Ocean (Lauretano et al., 2015), and a bulk sediment carbon isotope record from ODP Site 1262 (Zachos et al., 2010; Littler et al., 2014), Walvis Ridge, to investigate coeval carbon isotope change and registration of multiple CIEs in the different carbonate proxies. Finally, we investigate one recently proposed mechanism for terrestrial amplification of CIEs in an attempt to explain the observed early Eocene carbon isotope excursions in paleosol carbonate.

2 Material and methods

Pedogenic carbonate nodules were sampled at 12.5 cm spacing where present after removal of the weathered surface in the West Branch and Creek Star Hill sections located in the McCullough Peaks area of the northern Bighorn Basin, Wyoming (USA; Fig. 1). Sediment samples from soil-B horizons for reconstruction of Mean Annual Precipitation (MAP) are from the same sections and from the Upper Deer Creek section of Abels et al. (2012).

Micritic parts of the nodules were cleaned and ground to powder, while spar was taken out after crushing the nodule in few pieces. Carbon isotope ratios of carbonate micrite were measured using a SIRA-24 isotope ratio mass spectrometer of VG (vacuum generators) at Utrecht University (Netherlands). Prior to analysis, samples were roasted at 400 °C under vacuum before reaction with dehydrated phosphoric acid in a common-bath system for series of 32 samples and 12 standards. Carbon isotope ratios are reported as $\delta^{13}\text{C}$ values, where $\delta^{13}\text{C} = (R_{\text{sample}}/R_{\text{standard}} - 1)$, reported in per mil units (‰), and the standard is VPDB. These isotope ratio measurements are normalized based on repeated measurements of in-house powdered carbonate standard (NAXOS) and analytical precision was calculated from inclusion of three IAEA-CO1 standards in every series of 32 samples. Analytical precision is ± 0.1 ‰ for $\delta^{13}\text{C}$ (1 σ), whereas variability within individual paleosols averaged 0.2 ‰.

Title Page

Abstract

Introduction

Conclusions

References

Tables

Figures



Back

Close

Full Screen / Esc

Printer-friendly Version

Interactive Discussion



Carbon isotope excursions in paleosol carbonate

H. A. Abels et al.

Title Page

Abstract

Introduction

Conclusions

References

Tables

Figures



Back

Close

Full Screen / Esc

Printer-friendly Version

Interactive Discussion



To calculate CIE magnitudes, carbon isotope records are first detrended to exclude the influence of the long term Paleocene to early Eocene trends. The CIE magnitudes are then calculated as the difference between pre-excursion carbon isotope values and excursion values within the core of the main body (Table 1; Supplement). Standard errors are calculated using variability in background and excursion values. Standard errors of marine CIEs are small, partially possibly because of the relatively low amount of data showing little variability, and in Fig. 4 therefore larger, potentially more realistic standard errors are plotted of 0.4 for larger and 0.3‰ for smaller events.

We evaluated the potential effect of $p\text{CO}_2$ -induced changes in plant photosynthetic carbon isotope discrimination (Δ_p) on the scaling of pedogenic carbonate CIEs. For this, we used experimentally determined $\Delta_p/p\text{CO}_2$ relationships to estimate changes in Δ_p for each hyperthermal under a range of assumed initial conditions and severities of CO_2 change. Our calculations used the hyperbolic response form observed by Schubert and Jahren (2012) and adopted the parameter values determined by those authors for a multi-taxonomic synthesis of experimental data:

$$\Delta_p = 5.93 \times (p\text{CO}_2 + 25) / (28.26 + 0.21 \times (p\text{CO}_2 + 25)) \quad (1)$$

This equation was first used to estimate pre-event Δ_p values using a range of assumed background latest Paleocene – early Eocene $p\text{CO}_2$ values ($p\text{CO}_{2,i}$) from 500 to 1500 ppmv. Although background $p\text{CO}_2$ was likely not static through the time interval considered here, current paleo- $p\text{CO}_2$ proxy data do not clearly resolve changes at a level that could be incorporated in the modeling, and for the current analysis we conservatively assume a fixed background condition across all events. We then calculated peak-event Δ_p values for each hyperthermal assuming that the $p\text{CO}_2$ increase during each event ($\Delta p\text{CO}_2$) was a linear function of the magnitude of the event's CIE, as recorded in the Walvis Ridge benthic record ($\text{CIE}_{\text{benth}}$):

$$\Delta p\text{CO}_{2,h} = p\text{CO}_{2,i} + \Delta p\text{CO}_{2,\text{PETM}} \times \text{CIE}_{\text{benth,h}} / \text{CIE}_{\text{benth,PETM}}, \quad (2)$$

where h is an early Eocene hyperthermal event and a range of values for $p\text{CO}_2$ increase during the PETM, $\Delta p\text{CO}_{2,\text{PETM}}$, from 500 to 1500 ppmv were considered. Al-

though a recent study suggested a somewhat higher value for $\Delta p\text{CO}_{2,\text{PETM}}$ (Meissner et al., 2014; Cui et al., 2011; Kiehl and Shields, 2013) the range considered here spans most other estimates (Zeebe et al., 2009; Cui et al., 2011; Bowen, 2013) and consideration of larger changes would not alter the main conclusions drawn from this work below.

3 Results

3.1 Bighorn Basin

High-resolution pedogenic carbonate carbon isotope records are constructed for the lower Eocene of the Willwood Formation in the McCullough Peaks area, northern Bighorn Basin, Wyoming (USA; Fig. 1). Previous work included the Upper Deer Creek (UDC) section, where the carbon isotope excursions of ETM2 and H2 hyperthermal events were located (Abels et al., 2012). Here, we analyze two parallel sections, the Creek Star Hill (CSH) and West Branch (WB) sections, separated by 1 to 2 km from the UDC section (Fig. 1). The isotope record is extended upwards in the WB section and downwards in the Deer Creek Amphitheater section (DCA; Abels et al., 2013). We construct a composite stratigraphic section by connecting the four sections via lateral tracing of marker beds in the field, such as the P1 to P8 purple soils in the ETM2-H2 stratigraphic interval (Abels et al., 2012).

The carbon isotope record of paleosol carbonate of the McCullough Peaks (MCP) composite section shows four carbon isotope excursions (CIEs; Fig. 2). The lower excursions of ~ 3.8 and ~ 2.8 ‰ in magnitude (see methods for CIE magnitude calculation) have previously been related to the ETM2/H1 and H2 events (Abels et al., 2012) and are shown to be similar in the parallel Upper Deer Creek, West Branch, and Creek Star Hill sections. This confirms the presence and regional preservation of these CIEs in the Willwood Formation. The two younger carbon isotope excursions are ~ 2.4 and ~ 1.6 ‰ in magnitude and both located in the West Branch section (Fig. 2). These ex-

Carbon isotope excursions in paleosol carbonate

H. A. Abels et al.

Title Page

Abstract

Introduction

Conclusions

References

Tables

Figures



Back

Close

Full Screen / Esc

Printer-friendly Version

Interactive Discussion



cursions likely relate to the CIEs of the I1 and I2 events that occur in the subsequent 405 kyr eccentricity maximum after ETM2/H1 and H2 (Cramer et al., 2003).

Besides these CIEs, several intervals show less-well-defined light carbon isotopes excursions of $\sim 0.5\text{--}1\text{‰}$; two below ETM2 at MCP meter levels 95 and 145 and two above H2 at meter levels ~ 260 and ~ 290 , and one above I2 at meter 400. This scale of variability is harder to detect as the carbon isotopes show background variability of $\sim 1\text{‰}$ (2σ), possibly noise related to local environmental factors. The spacing between the CIEs and the low amplitude variability in the MCP section is on average ~ 34 m. Bandpass filtering of this scale of variability specifically shows a strong coherent variation through the ETM2 to I2 interval (Fig. 3).

Precession-forcing of overbank-avulsion lithological cyclicity in the Willwood Formation was recently substantiated with data from the Deer Creek Amphitheater section (Abels et al., 2013). In the DCA section, the cyclicity occurs at a scale of ~ 7.1 m. In the three sections now covering ETM2-H2, the cyclicity has a very similar average thickness of 7.06 m. The precession cyclicity comprises heterolithic sandy intervals showing little pedogenic imprint alternating with mudrock intervals showing intense pedogenesis. In the precession forcing sedimentary synthesis, the heterolithic intervals are related to periods of regional avulsions and rapid sedimentation, while the mudrocks are related to periods of overbank sedimentation when the channel belt had a relatively stable position (Abels et al., 2013). This scale of sedimentary cyclicity is also observed higher in the West Branch section. Average climatic precession cycles in the Eocene last ~ 20 kyr resulting in ~ 7.1 m of sediment. This gives an average sedimentation rate of ~ 0.35 m kyr⁻¹, resulting in ~ 96 kyr for the 34 m cyclicity observed in the carbon isotope records in the ETM2-I2 interval. This is in line with ~ 100 kyr eccentricity forcing of individual hyperthermals and a 405 kyr eccentricity forcing of the ETM2-H2 and I1-I2 couples.

We produce mean annual precipitation (MAP) estimates across the ETM2-I2 interval with the CALMAG method that uses bulk oxide ratios in soil-B horizons (Nordt and Driese, 2010). Soil-B horizons thicker than 1 m should ideally be used for this proxy

Carbon isotope excursions in paleosol carbonate

H. A. Abels et al.

Title Page

Abstract

Introduction

Conclusions

References

Tables

Figures



Back

Close

Full Screen / Esc

Printer-friendly Version

Interactive Discussion



et al., 2005; Kraus et al., 2013). This would suggest that the regional climatic and/or environmental response to the PETM differed from the post-PETM hyperthermals.

Besides precipitation, temperature, vegetation, and sediment type and rates also have a large impact on soil moisture and changes in CALMAG geochemical data should be considered in light of changes in these factors (Kraus et al., 2013). For the four younger hyperthermals, there are no temperature or vegetation data available, while the impact of sediment type and rates needs to be investigated for all five hyperthermals. It thus remains uncertain whether the observed opposite CALMAG changes between PETM and the four post-PETM hyperthermals relate to opposite precipitation trends or environmental (depositional) trends.

The precession forcing of the 7 m thick overbank-avulsion sedimentary cycles (Abels et al., 2013) is in line with ~ 100 and 405 kyr eccentricity forcing of the carbon cycle changes in the ETM2 to I2 stratigraphic interval (Fig. 3). Mudrock intervals with well-developed purple and purple-red paleosols occur predominantly in the eccentricity maxima, while the minima seem to be rich in sand. This could point to a more prolonged relatively stable position of the channel belt on the floodplain, causing less coarse clastic deposition on the floodplains, during eccentricity maxima (Abels et al., 2013). Such an effect could have occurred in combination with or due to more intense pedogenesis under warmer and wetter climates. However, in this interval, the eccentricity-related change is dominated by the hyperthermal events and corroboration of the eccentricity impact is needed from an interval lacking hyperthermals.

4.2 Marine-terrestrial correlations

The benthic carbon isotope record of the I1 and I2 events at Site 1263 reveal very similar patterns as in the bulk and benthic carbon isotope record of Site 1262 (Zachos et al., 2010; Littler et al., 2014) at both eccentricity and precession time scales, as was indicated previously for ETM2 and H2 (Stap et al., 2009). These records even capture very detailed features such as the short-term pre-ETM2 and pre-H2 excursions, and a similar pattern in the I2 excursion. These patterns were clearly driven by changes in

CPD

11, 1857–1885, 2015

Carbon isotope excursions in paleosol carbonate

H. A. Abels et al.

Title Page

Abstract

Introduction

Conclusions

References

Tables

Figures



Back

Close

Full Screen / Esc

Printer-friendly Version

Interactive Discussion



the carbon isotope ratio of the atmosphere–ocean exogenic carbon pool as related to precession forcing (Stap et al., 2009).

Some of these precession-scale details are also captured by the pedogenic carbonate carbon isotope record from the Bighorn Basin suggesting their global nature (Fig. 3). A pre-ETM2 excursion occurs in the McCullough Peaks composite at meter 183, while the shape of the I2 excursion is remarkably similar to the marine records. Main differences on these depth scale plots are the relative expanded CIE intervals and short recovery phases between H1 and H2 and between I1 and I2 in the Bighorn Basin with respect to the Atlantic Ocean records. Sediment accumulation rates were influenced by carbonate dissolution in the events and carbonate overshoot after the events in the marine realm. At the same time, in the Bighorn Basin sedimentation rates might have been higher during the events due to increased sediment budgets and subsequently lower during their recovery phases. These processes might cause the expanded CIEs and contracted recovery phases in the Bighorn Basin with respect to the marine records when comparing on depth scale.

4.3 Marine carbon isotope excursions

Deciphering the true scale and timing of ocean–atmosphere $\Delta\delta^{13}\text{C}$ during hyperthermal events is principally hampered by environmental impacts on carbon isotope fractionation between marine and terrestrial substrates and their proxies (Sluijs and Dickens, 2012). We compare the magnitudes of the CIEs of PETM, ETM2 (H1), H2, I1 and 2 in bulk carbonate and benthic foraminiferal carbon isotope records of Sites 1262 and 1263 at Walvis Ridge, Atlantic Ocean, and pedogenic carbonate in the Bighorn Basin, Wyoming (see methods for CIE magnitude calculations; Table 1).

An approximately linear scaling is found between bulk carbonate and benthic foraminiferal carbonate carbon isotope excursion magnitudes of the five Paleocene–Eocene hyperthermal events (Fig. 4). The bulk sediment and benthic foraminiferal CIEs have different values for the hyperthermals because these proxies react differently to the carbon addition to the ocean water, resulting in dissolution and pH

Carbon isotope excursions in paleosol carbonate

H. A. Abels et al.

Title Page

Abstract

Introduction

Conclusions

References

Tables

Figures



Back

Close

Full Screen / Esc

Printer-friendly Version

Interactive Discussion



changes effecting isotope discrimination in the different carbonate phases (Uchikawa and Zeebe, 2010). An approximate scaling between CIEs in the two different marine proxy records would suggest proportionality between the severity of local palaeoenvironmental changes, which cause the differences between the CIEs in the two proxies, and the amount of isotopically-light carbon added to the ocean-atmosphere system (Abels et al., 2012). That could imply that atmospheric $p\text{CO}_2$ change, as a primary forcer of paleoenvironmental change, scaled approximately linearly with CIE magnitude across the five events, and that the isotopic composition of the carbon and probably the carbon source(s) were similar for the five hyperthermals. This would argue against the proposed dichotomy of causes for the PETM compared to the smaller younger hyperthermals (e.g. Sexton et al., 2011), in line with previous results showing proportional scaling of oxygen vs. carbon isotope change in deep-sea benthic foraminifera for the PETM, ETM2, and H2 events (Stap et al., 2010a). Alternatively, the PETM carbon sources and isotope-signatures were different and not scaled between the events. Then, the approximate scaling of the CIEs in the two proxy records of all five events should have resulted in different environmental impact on isotope change in the bulk and benthic carbonate phases in the two sites leveling the CIEs to the linear scaling. This would imply that environmental change in the Bighorn Basin was probably not scaled between the five events.

4.4 Terrestrial carbon isotope excursions

Comparing CIEs in paleosol carbonate of the Bighorn Basin with bulk sediment or benthic foraminiferal carbonate at Walvis Ridge Sites 1262 and 1263, respectively, reveals an approximately linear change across the ETM2, H2, and I1 and I2 events (Fig. 4). In contrast to a previous comparison based only on data from the PETM, ETM2, and H2 (Abels et al., 2012), the observed relationship for the post-PETM hyperthermals converges on the origin, consistent with expectations if the terrestrial and marine CIEs reflect a common change in atmosphere/ocean $\delta^{13}\text{C}$ plus local environmental effects that scale in severity with CIE magnitude. Extrapolation of this approximately linear

Carbon isotope excursions in paleosol carbonate

H. A. Abels et al.

Title Page

Abstract

Introduction

Conclusions

References

Tables

Figures



Back

Close

Full Screen / Esc

Printer-friendly Version

Interactive Discussion



relationship shows that the magnitude of the PETM CIE is reduced in paleosol carbonate with respect to the scaling relationship and observed marine carbonate values (Fig. 4). Using comparison with benthic foraminiferal carbonate CIEs, the anomaly of the PETM CIE magnitude in paleosol carbonate is 3.6‰. Using bulk sediment CIEs, the anomaly is 2.1‰. These likely represent underestimates of the true marine CIE, as records based on analyses of mixed-layer planktonic forams at marine sites where dissolution was minimal show a slightly larger CIE, closer to 4.0‰. (e.g., Zachos et al., 2007). For the ETM2 and 3 events, even though planktonic records are sparse, or still non-existent, given the lack of extensive solution, we would anticipate only minor difference in the magnitude of the CIE between benthics and planktonics. In other words, the use of benthic rather than planktonic foraminifer $\delta^{13}\text{C}$ records would not explain the marine/terrestrial scaling differences between PETM and subsequent events.

Differences in terrestrial and marine CIE magnitudes for the PETM have previously been explained by a range of different environmental factors causing changes in plant and soil system carbon isotope fractionation with respect to the atmospheric carbon isotope excursion (Bowen et al., 2004; Smith et al., 2007). Among the factors influencing the terrestrial CIE signals are temperature effects on carbon isotope fractionation and changes in ecosystem productivity and organic matter turnover rates (Bowen et al., 2004). As argued above, linear scaling of marine bulk carbonate and benthic foraminiferal records for the same five CIEs might indicate that carbon sources were similar and amount of carbon input linearly scaled with CIE magnitude among the five events. If environmental change in the Bighorn Basin was proportional to atmospheric CO_2 increase, the environmental change may also have been proportional to CIE magnitude across the five events. This might imply CIE-proportional changes in temperature, ecosystem productivity, and organic matter turnover effects on the terrestrial carbon isotope records, and thus changes in marine-terrestrial CIE magnitude offsets that increased proportionally with CO_2 increase and “global” CIE magnitude. Data from the four younger hyperthermals appear to define a common CIE scaling relationship that could be explained in terms of this reasoning, in which case reconciling the lower rel-

CPD

11, 1857–1885, 2015

Carbon isotope excursions in paleosol carbonate

H. A. Abels et al.

[Title Page](#)

[Abstract](#)

[Introduction](#)

[Conclusions](#)

[References](#)

[Tables](#)

[Figures](#)



[Back](#)

[Close](#)

[Full Screen / Esc](#)

[Printer-friendly Version](#)

[Interactive Discussion](#)



ative magnitude of the PETM CIE in paleosol carbonate with the data from the other events requires unique local environmental forcing during the PETM possibly including a non-linear component, or that the PETM was fuelled by different carbon sources resulting in different isotope-signature vs. size of the carbon input.

5 Recently, Schubert and Jahren (2012) presented data that show exponentially reduced carbon isotope fractionation of C_3 photosynthesizing plants under increasing pCO_2 . We use their experimental results to test the potential role of reduced carbon isotope fraction under increased pCO_2 as a non-linearly-scaling environmental factor that might reconcile CIE data from the five hyperthermals. Estimates for both pre-PETM
10 atmospheric pCO_2 and the CO_2 addition during the PETM remain matter of debate (Meissner et al., 2014). Therefore, we estimate impact of the exponentially decreasing carbon isotope fractionation on a range of initial pCO_2 values and a range of CO_2 increases during the PETM. For the PETM, we find a model-estimated land plant CIE, calculated as benthic foraminiferal CIE plus the increase in photosynthetic discrimina-
15 tion, that is in line with observed n-alkane CIE of 4.2‰ at high background pCO_2 and relatively low added CO_2 (Fig. 5a).

We then estimate changes in photosynthetic fractionation for each of the four post-PETM events under each scenario of background pCO_2 and PETM pCO_2 change. This is done with the assumption that the change in pCO_2 during each event was equal to the PETM pCO_2 change times the ratio of the benthic CIE for that event to the benthic CIE for the PETM. The estimated terrestrial CIE for each post-PETM event is then
20 equal to the benthic CIE plus the change in photosynthetic discrimination. Then, the relationship between these modeled estimates and the observed Bighorn Basin pedogenic carbonate estimates was linearly extrapolated to calculate what the magnitude of the PETM CIE in pedogenic carbonate should have been, if it scaled linearly with
25 respect to the other events, after correcting for photosynthetic discrimination change.

Comparison of these model-derived PETM CIE magnitudes with the observed data shows that nowhere in the explored parameter space can the discrimination response come close to reconciling the observed PETM CIE magnitude with the pseudo-linear

Carbon isotope excursions in paleosol carbonate

H. A. Abels et al.

[Title Page](#)[Abstract](#)[Introduction](#)[Conclusions](#)[References](#)[Tables](#)[Figures](#)[Back](#)[Close](#)[Full Screen / Esc](#)[Printer-friendly Version](#)[Interactive Discussion](#)

marine-terrestrial scaling relationship observed for the other CIEs. The photosynthetic fractionation response comes closest to providing a solution in cases where the background $p\text{CO}_2$ is relatively low and the PETM $p\text{CO}_2$ change relatively high (lower right part of the panel). However, for these conditions the modeled change in photosynthetic fractionation is a poor match to observed n-alkane data for the PETM (Fig. 5a).

The model estimates are presented here using the benthic foraminiferal CIEs as a proxy for global atmospheric carbon isotope change, as these are likely a better approximation of the atmospheric CIEs than the bulk carbonate (Kirtland Turner and Ridgwell, 2013). Using the bulk sediment CIEs, the solutions are little better (not shown), and nowhere in the parameter space does the model satisfy the constraints from the PETM n-alkane data and also reconcile the observed PETM pedogenic carbonate CIE with the linear scaling observed for the other events to within better than $\sim 2\%$. In conclusion, our model results indicate that the reduction of carbon isotope fractionation in plants cannot explain the observed difference in terrestrial-marine CIE scaling for the PETM relative to the subsequent hyperthermals.

If the hypothesis of a common carbon source and CIE-proportional climatic change across the five events is correct (Stap et al., 2010a) then our analysis suggests a component of PETM Bighorn Basin environmental change that was not linearly proportional to CIE magnitude, perhaps due to the crossing of Earth system thresholds during this largest hyperthermal event. Our proxy estimates indeed suggest a different response of soil moisture (Fig. 2) during the PETM than during the four younger and smaller hyperthermals. The indication of soil drying during the PETM (Kraus and Riggins, 2007; Kraus et al., 2013), whereas the ETM2-I2 data show unchanged or slightly increased soil moisture levels during these events, may suggest differential environmental response that modulated Bighorn Basin carbon cycling and carbon isotope fractionation across these events. Such soil moisture differences between the PETM and younger hyperthermals could also have led to distinct plant community changes affecting the respective CIEs in pedogenic carbonate (Smith et al., 2007). In case the PETM was not scaled to the other events, the dampened terrestrial CIE of the PETM would be

Carbon isotope excursions in paleosol carbonate

H. A. Abels et al.

[Title Page](#)[Abstract](#)[Introduction](#)[Conclusions](#)[References](#)[Tables](#)[Figures](#)[Back](#)[Close](#)[Full Screen / Esc](#)[Printer-friendly Version](#)[Interactive Discussion](#)

more easily explained by heavier sources of carbon with respect to the younger hyperthermals.

5 Conclusions

We recovered the carbon isotope excursions related to the I1 and I2 events in floodplain sedimentary records from the Bighorn Basin, Wyoming. This adds to the three earlier found CIEs, the PETM, ETM2, and H2, underlining the sensitivity of these floodplain records for recording global atmospheric changes. Correlations with marine records and eccentricity-forcing of hyperthermals corroborate the continuity of sedimentation that occurred in the basin starting above precession time scales of ~ 20 kyr. Our CAL-MAG proxy-based soil moisture estimates reproduce similar or slightly enhanced soil moisture contents for the younger four hyperthermals, in contrast to reconstructions for the PETM. More environmental reconstructions, such as from vegetation, are needed for these four younger hyperthermals in the Bighorn Basin to confirm such a difference.

Comparison of the CIE magnitudes between bulk sediment and benthic foraminiferal carbonate at Walvis Ridge, southern Atlantic Ocean, shows an approximately linear relation among these five events. As the CIEs in different carbonate proxies are dependent on environmental factors that in their turn depend on the size of the carbon input into the atmosphere, this could suggest the magnitudes of these five CIEs were linearly scaled to the amount of carbon added to the exogenic carbon pool and that environmental change was similar and scaled proportional to the CIE magnitude as well. Alternatively, the PETM carbon sources and isotope-signatures were not similar to the younger events and the approximate scaling of the five CIEs including the PETM resulted from different environmental impact on isotope change by coincidence leveling the CIEs in the two distinct proxies from different water depths to a linear scaling.

Comparison of the Bighorn Basin pedogenic carbonate CIEs with the marine benthic foraminiferal CIEs shows an approximately linear relation for the four smaller hyperthermals, whereas the CIE in pedogenic carbonate of the PETM appears reduced in

Carbon isotope excursions in paleosol carbonate

H. A. Abels et al.

Title Page

Abstract

Introduction

Conclusions

References

Tables

Figures



Back

Close

Full Screen / Esc

Printer-friendly Version

Interactive Discussion



magnitude by 2–4‰ relative to that relationship. Reduction of carbon isotope fractionation by C₃ land plants in response to pCO₂ change cannot fully explain this pattern in isolation. Additional, likely soil-process-related and plant community changes, would be needed to explain the observed pattern, if indeed the PETM had an impact on carbon budgets and climate that scaled with CIE magnitude similarly to the younger hyperthermals. The magnitude of carbon isotope excursions in pedogenic carbonate is a function of many atmospheric, climatic, biotic, and sedimentary variables, showing that its use for environmental reconstruction can be complex, while the stratigraphic significance again reveals striking.

The Supplement related to this article is available online at doi:10.5194/cpd-11-1857-2015-supplement.

Acknowledgements. H. A. Abels acknowledges NWO-ALW for VENI grant 863.11.006. Will Clyde, Jerry Dickens, Frits Hilgen, Jelmer Laks, and Appy Sluijs are thanked for discussions, Arnold van Dijk, David Ecclestone, Jori Jansen, Sophie van Olst, Christine Satter, and Petra Zaal for laboratory assistance, and the Churchill family of Powell, Wyoming, Peter van den Berg, Francien van den Berg, Matthew Gingerich, Marijn Koopman, Jort Koopmans, Sander Smeets, and Karel Steensma for field assistance.

References

- Abels, H. A., Clyde, W. C., Gingerich, P. D., Hilgen, F. J., Fricke, H. C., Bowen, G. J., and Lourens, L. J.: Terrestrial carbon isotope excursions and biotic change during Palaeogene hyperthermals, *Nat. Geosci.*, 5, 326–329, 2012.
- Abels, H. A., Kraus, M. J., and Gingerich, P. D.: Precession-scale cyclicity in the fluvial lower Eocene Willwood Formation of the Bighorn Basin, Wyoming (USA), *Sedimentology*, 60, 1467–1483, doi:10.1111/sed.12039, 2013.

Carbon isotope excursions in paleosol carbonate

H. A. Abels et al.

Title Page

Abstract

Introduction

Conclusions

References

Tables

Figures



Back

Close

Full Screen / Esc

Printer-friendly Version

Interactive Discussion



Carbon isotope excursions in paleosol carbonate

H. A. Abels et al.

Title Page

Abstract

Introduction

Conclusions

References

Tables

Figures



Back

Close

Full Screen / Esc

Printer-friendly Version

Interactive Discussion



Adams, J. S., Kraus, M. J., and Wing, S. L.: Evaluating the use of weathering indices for determining mean annual precipitation in the ancient stratigraphic record, *Palaeogeogr. Palaeoclimatol.*, 309, 358–366, 2011.

Bowen, G. J.: Up in smoke: a role for organic carbon feedbacks in Paleogene hyperthermals, *Global Planet. Change*, 109, 18–29, 2013.

Bowen, G. J. and Bowen, B. B.: Mechanisms of PETM global change constrained by a new record from central Utah, *Geology*, 36, 379–382, 2008.

Bowen, G. J., Koch, P. L., Gingerich, P. D., Norris, R. D., Bains, S., and Corfield, R. M.: Refined isotope stratigraphy across the continental Paleocene–Eocene boundary on Polecat Bench in the Northern Bighorn Basin, in: *Paleocene–Eocene Stratigraphy and Biotic Change in the Bighorn and Clark Fork Basins, Wyoming*, edited by: Gingerich, P. D., University of Michigan Papers on Paleontology, Ann Arbor, Michigan, USA, 33, 73–88, available at: <http://hdl.handle.net/2027.42/48328>, 2001.

Bowen, G. J., Beerling, D. J., Koch, P. L., Zachos, J. C., and Quattlebaum, T.: A humid climate state during the Paleocene–Eocene Thermal Maximum, *Nature*, 432, 495–499, 2004.

Bowen, G. J., Maibauer, B. J., Kraus, M. J., Röhl, U., Westerhold, T., Steimke, A., Gingerich, P. D., Wing, S. L., and Clyde, W. C.: Two massive, rapid releases of carbon during the onset of the Palaeocene–Eocene Thermal Maximum, *Nat. Geosci.*, 8, 44–47, 2015.

Chen, Z., Ding, Z., Tang, Z., Wang, X., and Yang, S.: Early Eocene carbon isotope excursions: evidence from the terrestrial coal seam in the Fushun Basin, Northeast China, *Geophys. Res. Lett.*, 41, 3559–3564, doi:10.1002/2014GL059808, 2014.

Cramer, B. S., Wright, J. D., Kent, D. V., and Aubry, M.-P.: Orbital climate forcing of $\delta^{13}\text{C}$ excursions in the late Paleocene–early Eocene (chrons C24n–C25n), *Paleoceanography*, 18, 1097, doi:10.1029/2003PA000909, 2003.

Cui, Y., Kump, L. R., Ridgwell, A. J., Charles, A. J., Junium, C. K., Diefendorf, A. F., Freeman, K. H., Urban, N. M., and Harding, I. C.: Slow release of fossil carbon during the Palaeocene–Eocene Thermal Maximum, *Nat. Geosci.*, 4, 481–485, 2011.

Dickens, G.R., O’Neil, J. R., Rea, D. K., and Owen, R. M.: Dissociation of oceanic methane hydrate as a cause of the carbon isotope excursion at the end of the Paleocene, *Paleoceanography*, 10, 965–971, 1995.

Diefendorf, A. F., Mueller, K. E., Wing, S. L., Koch, P. L., and Freeman, K. H.: Global patterns in leaf ^{13}C discrimination and implications for studies of past and future climate, *P. Natl. Acad. Sci. USA*, 107, 5738–5743, 2010.

Carbon isotope excursions in paleosol carbonate

H. A. Abels et al.

[Title Page](#)[Abstract](#)[Introduction](#)[Conclusions](#)[References](#)[Tables](#)[Figures](#)[Back](#)[Close](#)[Full Screen / Esc](#)[Printer-friendly Version](#)[Interactive Discussion](#)

Hancock, H. J. L., Dickens, G. R., Strong, C. P., Hollis, C. J., and Field, B. D.: Foraminiferal and carbon isotope stratigraphy through the Paleocene–Eocene transition at Dee Stream, Marlborough, New Zealand, *New Zeal. J. Geol. Geop.*, 46, 1–19, 2003.

Hollis, C. J., Dickens, G. R., Field, B. D., Jones, C. M., and Strong, C. P.: The Paleocene–Eocene transition at Mead Stream, New Zealand: a southern Pacific record of early Cenozoic global change, *Palaeogeogr. Palaeoclimatol.*, 215, 313–343, 2005.

Kiehl, J. T. and Shields, C. A.: Sensitivity of the Palaeocene–Eocene Thermal Maximum climate to cloud properties, *Philos. T. R. Soc. A*, 371, 20130093, doi:10.1098/rsta.2013.0093, 2013.

Kirtland Turner, S. and Ridgwell, A.: Recovering the true size of an Eocene hyperthermal from the marine sedimentary record, *Paleoceanography*, 28, 1–13, doi:10.1002/2013PA002541, 2013.

Kraus, M. J. and Riggins, S.: Transient drying during the Paleocene–Eocene Thermal Maximum (PETM): analysis of paleosols in the bighorn basin, Wyoming, *Palaeogeogr. Palaeoclimatol.*, 245, 444–461, 2007.

Kraus, M. J., McInerney, F. A., Wing, S. L., Secord, R., Baczynski, A. A., and Bloch, J. I.: Paleohydrologic response to continental warming during the Paleocene–Eocene Thermal Maximum, Bighorn Basin, Wyoming, *Palaeogeogr. Palaeoclimatol.*, 370, 196–208, 2013.

Lauretano, V., Littler, K., Polling, M., Zachos, J. C., and Lourens, L. J.: Frequency, magnitude and character of hyperthermal events at the onset of the Early Eocene Climatic Optimum, *Clim. Past Discuss.*, accepted, 2015.

Littler, K., Röhl, U., Westerhold, T., and Zachos, J. C.: A high-resolution benthic stable-isotope record for the South Atlantic: implications for orbital-scale changes in Late Paleocene–Early Eocene climate and carbon cycling, *Earth Planet. Sc. Lett.*, 401, 18–30, 2014.

Lourens, L. J., Sluijs, A., Kroon, D., Zachos, J. C., Thomas, E., Röhl, U., Bowles, J., and Raffi, I.: Astronomical pacing of late Palaeocene to early Eocene global warming events, *Nature*, 435, 1083–1087, 2005.

McCarren, H., Thomas, E., Hasegawa, T., Röhl, U., and Zachos, J. C.: Depth dependency of the Paleocene–Eocene carbon isotope excursion: paired benthic and terrestrial biomarker records (Ocean Drilling Program Leg, 208, Walvis Ridge), *Geochem. Geophys. Geosyst.*, 9, Q10008, doi:10.1029/2008GC002116, 2008.

McInerney, F. A. and Wing, S. L.: The Paleocene–Eocene Thermal Maximum: a perturbation of carbon cycle, climate, and biosphere with implications for the future, *Annu. Rev. Earth Pl. Sc.*, 39, 489–516, 2011.

Carbon isotope excursions in paleosol carbonate

H. A. Abels et al.

Title Page

Abstract

Introduction

Conclusions

References

Tables

Figures



Back

Close

Full Screen / Esc

Printer-friendly Version

Interactive Discussion



Meissner, K. J., Bralower, T. J., Alexander, K., Dunkley Jones, T., Sijp, W., and Ward, M.: The Paleocene–Eocene Thermal Maximum: how much carbon is enough?, *Paleoceanography*, 29, 946–963, 2014.

Nicolo, M. J., Dickens, G. R., Hollis, C. J., and Zachos, J. C.: Multiple early Eocene hyperthermals: their sedimentary expression on the New Zealand continental margin and in the deep sea, *Geology*, 35, 699–702, 2007.

Schouten, S., Woltering, M., Rijpstra, W. I. C., Sluijs, A., Brinkhuis, H., and Sinninghe Damsté, J. S.: The Paleocene–Eocene carbon isotope excursion in higher plant organic matter: differential fractionation of angiosperms and conifers in the Arctic, *Earth Planet. Sc. Lett.*, 258, 581–592, 2007.

Sexton, P. F., Norris, R. D., Wilson, P. A., Pälike, H., Westerhold, T., Röhl, U., Bolton, C. T., and Gibbs, S.: Eocene global warming events driven by ventilation of oceanic dissolved organic carbon, *Nature*, 471, 349–353, 2011.

Sluijs, A. and Dickens, G. R.: Assessing offsets between the $\delta^{13}\text{C}$ of sedimentary components and the global exogenic carbon pool across early Paleogene carbon cycle perturbations, *Global Biogeochem. Cy.*, 26, GB4005, doi:10.1029/2011GB004224, 2012.

Smith, F. A., Wing, S. L., and Freeman, K. H.: Magnitude of the carbon isotope excursion at the Paleocene–Eocene Thermal Maximum: the role of plant community change, *Earth Planet. Sc. Lett.*, 262, 50–65, 2007.

Stap, L., Sluijs, A., Thomas, E., and Lourens, L. J.: Patterns and magnitude of deep sea carbonate dissolution during Eocene Thermal Maximum 2 and H2, Walvis Ridge, southeastern Atlantic Ocean, *Paleoceanography*, 24, PA1211, doi:10.1029/2008PA001655, 2009.

Stap, L., Lourens, L. J., Thomas, E., Sluijs, A., Bohaty, S., and Zachos, J. C.: High-resolution deep-sea carbon and oxygen isotope records of Eocene Thermal Maximum 2 and H2, *Geology*, 38, 607–610, 2010a.

Stap, L., Lourens, L., van Dijk, A., Schouten, S., and Thomas, E.: Coherent pattern and timing of the carbon isotope excursion and warming during Eocene Thermal Maximum 2 as recorded in planktic and benthic foraminifera, *Geochem. Geophys. Geosy.*, 11, Q11011, doi:10.1029/2010GC003097, 2010b.

Uchikawa, J. and Zeebe, R. E.: Examining possible effects of seawater pH decline on foraminiferal stable isotopes during the Paleocene–Eocene Thermal Maximum, *Paleoceanography*, 25, PA2216, doi:10.1029/2009PA001864, 2010.

Carbon isotope excursions in paleosol carbonate

H. A. Abels et al.

[Title Page](#)[Abstract](#)[Introduction](#)[Conclusions](#)[References](#)[Tables](#)[Figures](#)[Back](#)[Close](#)[Full Screen / Esc](#)[Printer-friendly Version](#)[Interactive Discussion](#)

- Zachos, J. C., Röhl, U., Schellenberg, S. A., Sluijs, A., Hodell, D. A., Kelly, D. C., Thomas, E., Nicolo, M., Raffi, I., Lourens, L. J., McCarren, H., and Kroon, D.: Rapid acidification of the ocean during the Paleocene–Eocene Thermal Maximum, *Science*, 308, 1611–1615, 2005.
- 5 Zachos, J. C., Bohaty, S. M., John, C. M., McCarren, H., Kelly, D. C., and Nielsen, T.: The Palaeocene–Eocene carbon isotope excursion: constraints from individual shell planktonic foraminifer records, *Philos. T. R. Soc. A*, 365, 1829–1842, doi:10.1098/rsta.2007.2045, 2007.
- Zachos, J. C., Dickens, G. R., and Zeebe, R. E.: An early Cenozoic perspective on greenhouse warming and carbon-cycle dynamics, *Nature*, 451, 279–283, 2008.
- 10 Zeebe, R. E., Zachos, J. C., and Dickens, G. R.: Carbon dioxide forcing alone insufficient to explain Palaeocene–Eocene Thermal Maximum warming, *Nat. Geosci.*, 2, 576–580, 2009.

Carbon isotope excursions in paleosol carbonate

H. A. Abels et al.

[Title Page](#)

[Abstract](#)

[Introduction](#)

[Conclusions](#)

[References](#)

[Tables](#)

[Figures](#)



[Back](#)

[Close](#)

[Full Screen / Esc](#)

[Printer-friendly Version](#)

[Interactive Discussion](#)



Table 1. Magnitudes of carbon isotope excursions for five Paleocene–Eocene hyperthermal events in paleosol carbonate of the Bighorn Basin, Wyoming (USA) and benthic foraminiferal and bulk sediment carbonate of Walvis Ridge Sites 1263 and 1262, Atlantic Ocean. Standard errors of the differences between detrended background variability and excursion variability are given (see Methods).

Event	Bighorn Basin CIE ped.carb.	st.error	Bighorn Basin CIE n-alkanes	st.error	Walvis Ridge Sites 1263/65 CIE ben.forams	st.error	Walvis Ridge Site 1262 CIE bulk carb.	st.error
PETM	5.90	0.86	4.23	0.67	3.38	0.12	1.93	0.08
EMT2/H1	3.78	0.56			1.30	0.18	0.89	0.05
H2	2.75	0.38			0.97	0.16	0.58	0.06
I1	2.42	0.45			0.88	0.16	0.63	0.07
I2	1.55	0.72			0.73	0.16	0.50	0.10

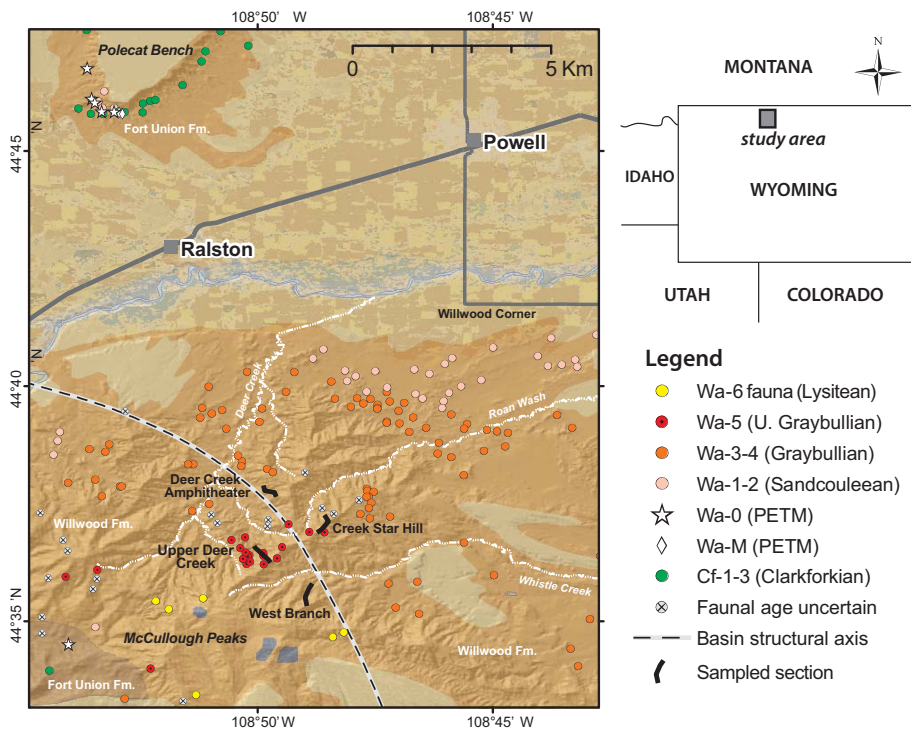


Figure 1. Location map of the sampling sites in the McCullough Peaks area of the northern Bighorn Basin in northeastern Wyoming (USA). Indicated are the fossil localities and their interpreted Wasatchian mammal zone and the four study sections. Polecat Bench in the northwest of the study sites is the location of the PETM.

Carbon isotope excursions in paleosol carbonate

H. A. Abels et al.

[Title Page](#)

[Abstract](#)

[Introduction](#)

[Conclusions](#)

[References](#)

[Tables](#)

[Figures](#)



[Back](#)

[Close](#)

[Full Screen / Esc](#)

[Printer-friendly Version](#)

[Interactive Discussion](#)



Carbon isotope excursions in paleosol carbonate

H. A. Abels et al.

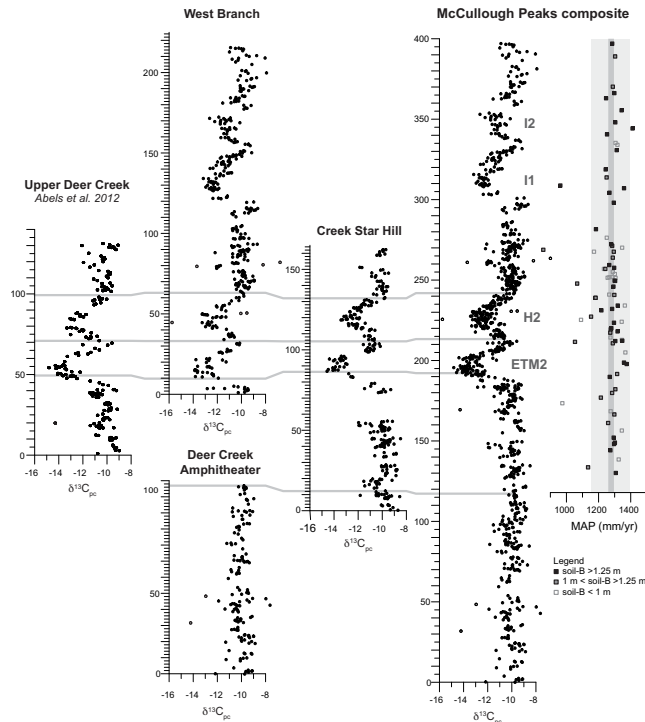


Figure 2. Carbon isotope stratigraphies of paleosol carbonate in the McCullough Peaks area, Bighorn Basin, Wyoming (USA). Shown are data from the Upper Deer Creek section of Abels et al. (2012), and the West Branch, Deer Creek Amphitheater, and Creek Star Hill sections. Grey horizontal lines represent field-based tracing of marker beds P1, P4, and P8 by which the McCullough Peaks composite carbon isotope stratigraphy has been constructed. To the right, Mean Annual Precipitation reconstructions from the CALMAG methods are given on the McCullough Peaks composite stratigraphy. Different symbols denote different thickness of the soil-B horizons. Note that there is no obvious change in soil moisture during the four hyperthermal events.

Title Page

Abstract

Introduction

Conclusions

References

Tables

Figures



Back

Close

Full Screen / Esc

Printer-friendly Version

Interactive Discussion



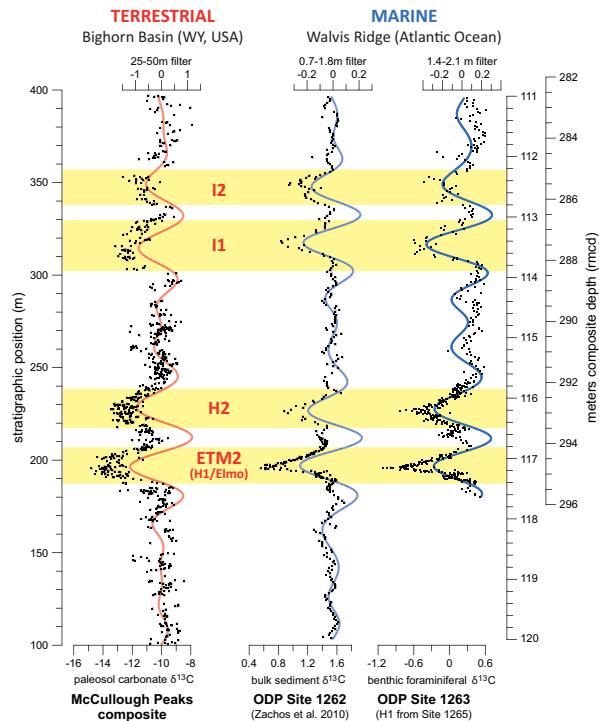


Figure 3. The McCullough Peaks paleosol carbonate carbon isotope stratigraphy compared in depth domain to the bulk sediment and benthic foraminiferal (*Nutallides truempyi*) carbon isotope stratigraphies at, respectively, ODP Site 1262 (Zachos et al., 2010) and 1263 (Stap et al., 2010a; this study) at Walvis Ridge in the southern Atlantic Ocean. Filters denote the ~ 100 kyr eccentricity band in the three records. Note that linear stretching of depth scales is sufficient to construct the figure indicating the constant average sedimentation rates at longer time scales in both realms. At smaller time scales, large sedimentation rate differences occur that in the marine realm relate to carbonate dissolution during and carbonate overshoot after the hyperthermal events.

Carbon isotope excursions in paleosol carbonate

H. A. Abels et al.

Title Page

Abstract

Introduction

Conclusions

References

Tables

Figures



Back

Close

Full Screen / Esc

Printer-friendly Version

Interactive Discussion



Carbon isotope excursions in paleosol carbonate

H. A. Abels et al.

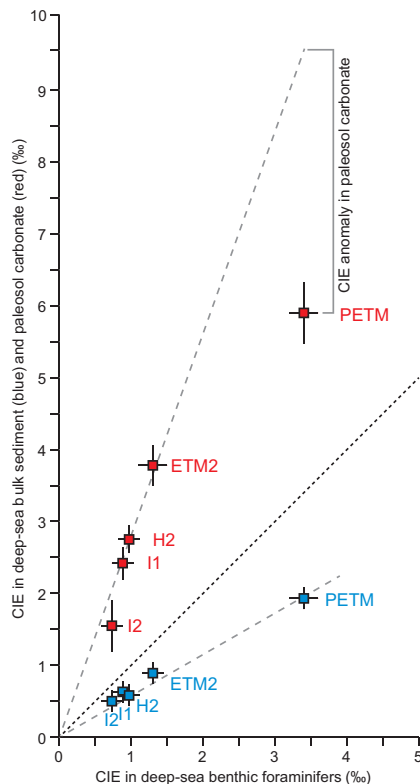


Figure 4. Carbon isotope excursions (CIEs) for the PETM, ETM2, H2, I1, and I2 events in the early Eocene compared between different proxies in marine and terrestrial settings. Blue squares denote benthic foraminiferal (x axis) vs. bulk sediment (y axis) CIEs at Walvis Ridge in the Atlantic Ocean. Red squares denote benthic foraminiferal (x axis) CIEs at Walvis Ridge vs. paleosol carbonate (y axis) CIEs in the Bighorn Basin, Wyoming (USA). Trendlines are forced through the origin. Note the apparent reduced CIE for the PETM in paleosol carbonate if extrapolation is used of the trendline through ETM2, H2, I1, and I2.

Title Page

Abstract

Introduction

Conclusions

References

Tables

Figures

◀

▶

◀

▶

Back

Close

Full Screen / Esc

Printer-friendly Version

Interactive Discussion



Carbon isotope excursions in paleosol carbonate

H. A. Abels et al.

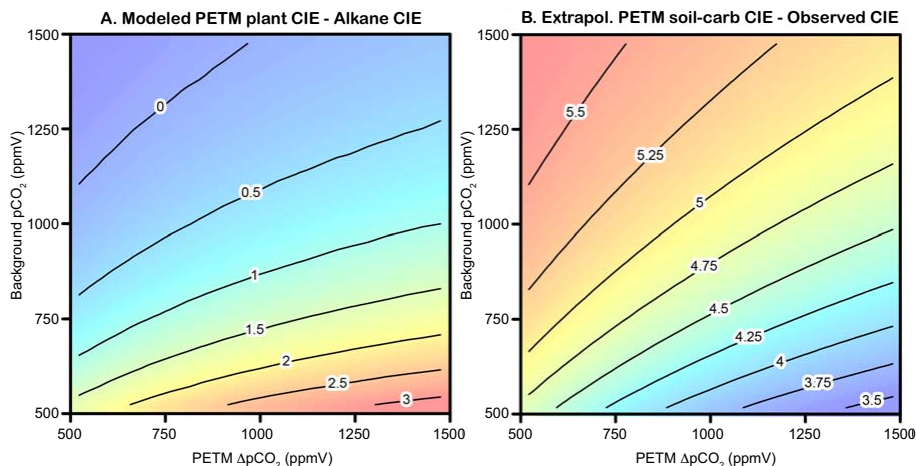


Figure 5. Calculated effects of changing photosynthetic carbon isotope fractionation on hyperthermal CIE magnitudes recorded in terrestrial substrates. **(a)** Difference between model-estimated terrestrial $\delta^{13}\text{C}$ change during the PETM, calculated as the magnitude of the observed benthic CIE plus the change in photosynthetic discrimination, and the magnitude of $\delta^{13}\text{C}$ change observed in Bighorn Basin n-alkane records (Table 1; Diefendorf et al., 2010). **(b)** Evaluation of the linearity of the marine/terrestrial CIE magnitude scaling after correction for modeled photosynthetic fractionation change. Plotted values are the difference between the PETM CIE magnitude predicted by extrapolating a linear least-squares relationship between observed pedogenic carbonate CIE magnitudes and photosynthesis-corrected benthic marine magnitudes ($\text{CIE}_{\text{benth,h}} + \Delta_{\text{p,h}}$) and the observed Bighorn Basin pedogenic carbonate CIE magnitude.

Title Page

Abstract

Introduction

Conclusions

References

Tables

Figures



Back

Close

Full Screen / Esc

Printer-friendly Version

Interactive Discussion

